Metabolomics screening identifies reduced L-carnitine to be associated with progressive emphysema.

Thomas M Conlon[1], Jörg Bartel[2], Korbinian Ballweg[1], Stefanie Günter[1], Cornelia Prehn[3], Jan Krumsiek[2], Silke Meiners[1], Fabian J. Theis[2], Jerzy Adamski[3,4,5], Oliver Eickelberg[1,6], and Ali Önder Yildirim[1,*]

[1]Comprehensive Pneumology Center, Institute of Lung Biology and Disease,
Helmholtz Zentrum München, Member of the German Center for Lung Research,
Ingolstädter Landstr. 1, 85764 Neuherberg, Germany.

[2]Institute of Computational Biology, Helmholtz Zentrum München,
Ingolstädter Landstr. 1, 85764 Neuherberg, Germany.

[3]Institute of experimental Genetics, Genome Analysis Center, Helmholtz Zentrum München,
Ingolstädter Landstr. 1, 85764 Neuherberg, Germany.

[4]German Center for Diabetes Research, Neuherberg, Germany.

[5]Chair for Experimental Genetics, Technical University of Munich, Freising-Weihenstephan, Germany.

[6]Klinikum der Universität München, Max-Lebsche-Platz 31, 81377 München, Germany.

Keywords: COPD, metabolome, biomarkers, apoptosis
Short title: L-carnitine attenuates emphysema

*Corresponding author:
Ali Önder Yildirim
oender.yildirim@helmholtz-muenchen.de

Abbreviations: BALF, bronchoalveolar-lavage fluid; C, carnitine; COPD, chronic obstructive pulmonary disease; H&E, hematoxylin and eosin; PC, phosphatidylcholine; PPE, porcine pancreatic elastase; SM, sphingomyelin.

Summary statement:
The progression of emphysema, a severe chronic lung disease, was found to be associated with reduced lung tissue specific L-carnitine in a clinically relevant mouse model. Furthermore, supplementing mice with this metabolite improved lung function and impaired disease progression.

Abstract

Chronic obstructive pulmonary disease (COPD) is characterized by chronic bronchitis, small airway remodeling and emphysema. Emphysema is the destruction of alveolar structures, leading to enlarged airspaces and reduced surface area impairing the ability for gaseous exchange.

To further understand the pathological mechanisms underlying progressive emphysema we used mass spectrometry–based approaches to quantitate the lung, bronchoalveolar-lavage fluid (BALF) and serum metabolome during emphysema progression in the established murine porcine pancreatic elastase (PPE) model on days 28, 56 and 161, compared to PBS controls. Partial Least Square analysis revealed greater changes in the metabolome of lung followed by BALF rather than serum during emphysema progression. Furthermore, we demonstrate for the first time that emphysema progression is associated with a reduction in lung specific L-carnitine, a metabolite critical for transporting long chain fatty acids into the mitochondria for their subsequent β-oxidation. *In vitro*, stimulation of the ATII-like LA4 cell line with L-carnitine diminished apoptosis induced by both PPE and H_2O_2. Moreover, PPE-treated mice demonstrated impaired lung function compared to PBS treated controls (lung compliance; 0.067±0.008ml/cmH_20 vs 0.035±0.005ml/cmH_20, $p<0.0001$), which improved following supplementation with L-carnitine (0.051±0.006, $p<0.01$) and was associated with a reduction in apoptosis.

In summary, our results provide a new insight into the role of L-carnitine and, importantly, suggest therapeutic avenues for COPD.

INTRODUCTION

Chronic obstructive pulmonary disease (COPD), a leading cause of chronic morbidity and mortality worldwide, is the result of long-term exposure to toxic gases and particles, in particular cigarette smoke, which drives excess mucus production, small airway remodeling, chronic bronchitis and emphysema (1). Emphysema is the destruction of septal tissue, leading to enlarged airspaces and reduced surface area (2). Historically, the underlying mechanism of emphysema has been viewed as a protease/anti-protease imbalance resulting in loss of the alveolar wall matrix (3), indeed patients with α1-antitrypsin deficiency have an increased risk of emphysema development (4). More recently, oxidative stress (5), accelerated senescence (6) and an apoptosis/proliferation imbalance of both alveolar epithelial and endothelial cells (7, 8) have been described responsible for the development of emphysema. These pathological changes result in a progressive airflow limitation that is not fully reversible. Indeed, there is no curative therapy for COPD, with currently available treatment only able to alleviate symptoms. Furthermore, little is known about the factors actually driving COPD disease progression towards a particular phenotype with progression amongst individual patients being highly variable.

Metabolomics, a rapidly expanding field which can be described as profiling the metabolic pathways of cells, offers a powerful tool for assessing the physiological state of an individual yielding a snapshot of cellular activities closer to the phenotype than simply gene expression (9). Thus providing, an invaluable resource for identifying new biomarkers of disease progression and further elucidating the underlying pathophysiological mechanisms of disease development, most importantly, to potentially reveal new therapeutic targets. To this end, there have been a number of studies published over the last few years assessing the COPD metabolome. This has included both untargeted (10-13) and targeted metabolomics (14) as well as a combination of both (15) either measured in plasma or serum from COPD patients. In their combined approach, Bowler et al. reported a strong inverse association between the level of some plasma sphingomyelins and emphysema in COPD patients (15). In addition to these clinical studies, one animal study used an untargeted approach to examine metabolomic changes in plasma following chronic exposure to cigarette smoke in a mouse model that resulted in emphysema (16), and a very recent study examining the effect of Traditional Chinese Medicine on a cigarette smoked induced rat model of COPD examined metabolite levels in lung tissue (17). However, to the best of our knowledge, no study has yet assessed the metabolomic changes occurring in the emphysematous lung during disease progression.

Here, for the first time, we use targeted metabolomics to assess changes in the metabolome locally to the lung and systemically in serum during disease progression, using the well-established porcine pancreatic elastase -induced model of murine emphysema (18, 19). We demonstrated that the progression of emphysema is associated with reduced levels of L-carnitine in the lung. L-carnitine's primary function is to transport long chain fatty acids into the mitochondria for their subsequent beta-oxidation and energy production (20), but is also a widely known anti-oxidant and protector against apoptosis (21-26). Interestingly, it has also been suggested following a randomized, double-blind trial that L-carnitine supplementation improved the control of asthma in children suffering from moderate persistent disease (27), which has been supported by an *in vivo* study in mice using the ovalbumin model of asthma tentatively reporting that L-carnitine treatment improved oxygen saturation and improved bronchial associated inflammation (28). Furthermore, L-carnitine supplementation as an ergogenic aid for COPD patients undergoing whole-body and respiratory muscle training programs demonstrated improved exercise tolerance and inspiratory muscle strength (29). However, a mechanism of action for the potential benefits of L-carnitine on lung pathology is also yet to be elucidated. To overcome these limitations and further investigate the interaction of metabolomics with the progression of emphysema development, we used mass spectrometry–based approaches to quantitate the lung, BALF and serum

metabolome at three different time points during emphysema progression. Furthermore, we integrate systems biological approaches with well-known metabolomics profiling to discover relationships that might elucidate mechanisms of progression in emphysema development. Therefore we hypothesized that supplementing mice with L-carnitine may protect against the development of PPE-induced emphysema. L-carnitine protected alveolar cells *in vitro* from PPE-induced apoptosis. Furthermore, supplementation of mice *in vivo* with L-carnitine prevented the development of alveolar apoptosis that is associated with emphysema and significantly improved the lung function of mice exposed to PPE. These findings suggest that L-carnitine supplementation, which is used clinically for the treatment of neonates with congenital metabolic diseases (30), may be beneficial to COPD patients.

MATERIALS AND METHODS

Animals

Female C57BL/6N mice (Charles River, Sulzfeld, Germany) aged 8-10 weeks were exposed oropharyngeally to a single application of 80U/Kg body weight PPE (Sigma-Aldrich, St. Louis, MO) in 80µl volume. Control mice were treated with 80µl PBS (Gibco, Life Technologies, Darmstadt, Germany). Mice were analyzed on d28, d56 and d161 for lung function, lung morphology and metabolomics profiling (n=6-11 per group). In further experiments mice were additionally treated every second day *i.p*. with 500mg/kg body weight L-carnitine (Sigma-Aldrich) and analyzed on d28 (n=4-6, experiment repeated twice). Mice were housed under specific pathogen free conditions, exposed to a 12hr light cycle with access to food and water *ad libitum*, in rooms maintained at a constant temperature and humidity. All animal experiments were performed according to strict governmental and international guidelines and were approved by the local government for the administrative region of Upper Bavaria.

Lung Function Measurement

Mice were anaesthetized with ketamine-xylazine, tracheostomized and their pulmonary function analysed using the flexiVent system (Scireq, Montreal, Canada). To obtain a mean lung volume similar to that of spontaneous breathing, mice were ventilated with a tidal volume of 10ml/kg at a frequency of 150 breaths/min. Lung mechanical properties were tested using the SnapShot and Primewave perturbations. Four readings per animal were taken.

Bronchoalvelar lavage fluid (BALF) and Serum

BALF was obtained for metabolomics analysis and to undertake total and differential cell counts for inflammatory cell recruitment of macrophages, neutrophils and lymphocytes. The lungs were lavaged with 3x500ul of PBS. Cells were pelleted at 400g, supernatant stored at -80°C for further analysis, and the cells resuspended in RPMI-1640 medium (Gibco, Life Technologies, Darmstadt, Germany) for the total cell count using a hemocytometer. Cytospins of the cell suspension were then prepared and stained using May-Grünwald-Giemsa for differential cell counting (200 cells/sample) using morphological criteria (31).

Serum was collected for metabolomics analysis. Mice were bled from the femoral artery, blood left to clot for several hours and then centrifuged at 1300g for 15min, serum was aliquoted and stored at -80°C for further analysis.

Lung Processing

The right lung was snap frozen in liquid nitrogen for further analysis. The left lung was fixed under a constant pressure of 20cm by intratracheal instillation of 6% paraformaldehyde and using systematic uniform random sampling embedded into paraffin for Hematoxylin and Eosin (H&E)-stained histological analysis and immunohistochemistry. Images of stained sections were obtained using a Mirax Desk (Carl Zeiss MicroImaging GmbH, Göttingen, Germany) slide scanner and analysed using Pannoramic Viewer version 1.15.2 (3DHistech Kft, Budapest, Hungary).

Quantitative Morphometry

H&E stained lung tissue sections were analysed by design-based stereology using an Olympus BX51 light microscope equipped with the new Computer Assisted Stereological Toolbox (newCAST, Visiopharm, Hoersholm, Denmark) as described previously (32). Air space enlargement was assessed by calculating the mean linear intercept (MLI) across 30 random fields of view per lung. Lung section images were

superimposed with a line grid, the intercepts of lines with alveolar septa and points hitting air space were counted to calculate the MLI, using MLI = $\sum P_{air}$ x L(p) / $\sum I_{septa}$ x 0.5. P_{air} are the points of the grid hitting air spaces, L(p) is the line length per point, I_{septa} is the sum of intercepts of alveolar septa with grid lines.

To quantify the percentage of caspase 3 positive alveolar epithelial cells the immunohistochemically stained lung tissue sections were also analysed using the newCAST system. 30 random fields of view per lung were taken and a frame grid superimposed on lung section images taken with the 40x objective. Within the frame, alveolar epithelial cells positive or negative for caspase 3 staining were counted and the percentage of positive alveolar epithelial cells was calculated.

Targeted Metabolomics

Targeted metabolomics screening using the Absolute*IDQ*™ p180 Kit (BIOCRATES Life Sciences AG, Innsbruck, Austria) followed by mass spectrometric analysis of serum, BALF and lung homogenate was undertaken by the Metabolomics Platform of the Genome Analysis Centre of the Helmholtz Zentrum München. For serum and BALF, 10 µL sample, for lung tissue 10 µL homogenate supernatant were applied to the kit plate. The tissue homogenate was prepared using a Precellys 24 homogenizer with an integrated cooling unit and homogenization tubes with ceramic beads (1.4 mm). To each mg of frozen lung tissue were added 3 µL of a dry ice cooled mixture of ethanol/phosphate buffer (85/15 v/v). The measurements with the Absolute*IDQ*™ kit p180 and the preparation of tissue samples have been previously described in detail (33, 34). Sample handling was performed with a Hamilton Microlab STAR™ robotics system (Hamilton Bonaduz AG, Bonaduz, Switzerland). Samples were analysed on an API4000™ LC/MS/MS system (AB Sciex Deutschland GmbH, Darmstadt, Germany). Data evaluation to quantify the metabolite concentrations was performed with the Met*IQ*™ software package, which is an integral component of the Absolute*IDQ*™ kit. Concentrations of all metabolites were calculated using internal standards and reported in µM. Further analyses on the data set were performed with MATLAB version 8.1.0.604 (R2013a; The MathWorks Inc., Nattick, MA) using the Statistics Toolbox version 8.2 and libPLS version 1.95 (35).

In total 186 metabolites are quantified by the kit: 40 acylcarnitines (Cx:y) including free carnitine (C0), 21 amino acids, 19 biogenic amines, 90 glycerophospholipids including lysophosphatidylcholines (lysoPC a Cx:y), diacylphosphatidylcholines (PC aa Cx:y) and acyl-alkyl phosphatidylcholines (PC ae Cx:y), 15 sphingolipids including sphingomyelins (SM Cx:y) and hydroxysphingomyelins (SM (OH) Cx:y), and hexose (sugars with 6 carbons). The abbreviation Cx:y is used to denote the lipid side chain composition, x and y refers to the total number of carbons and double bonds respectively, as the mass spectrometry technology used cannot distinguish between the side chains of diacylphospholipids. Acyl side chains are abbreviated with an “a”, alkyl and alkenyl residues with an “e”. Side chain substitutions are indicated as follows: hydroxy- (OH), methyl- (M) and dicarboxy- (DC).

L-carnitine quantification of lung tissue

Free L-carnitine levels were quantified in lung tissue using the L-Carnitine Assay Kit (Sigma-Aldrich, St. Louis, MO) as per manufacturer’s instructions. In brief, lung tissue was homogenized under liquid nitrogen using the Mikro-Dismembrator S (Sartorius AG, Göttingen, Germany) and extracted into Carnitine Assay Buffer. Reactions were prepared as described in the kit with each sample being analyzed in triplicate. To control for background readings from Coenzyme A, a blank sample omitting the Carnitine Converting Enzyme Mix was prepared. After incubation absorbance was measured at 570nm on a Microplate reader (Infinite M200 PRO NanoQuant, Tecan Deutschland GmbH, Crailsheim, Germany). L-

carnitine concentration was calculated from kit standards and normalized to the protein concentration as determined by the Pierce™ BCA protein Assay Kit (Thermo Fisher Scientific, Waltham, MA).

Immunohistochemistry

Paraffin embedded lung sections were first deparaffinized in xylene and rehydrated in alcohol before being treated with 1.8% (v/v) H_2O_2 solution (Sigma-Aldrich, St. Louis, MO) to block endogenous peroxidase activity. Heat induced epitope retrieval was undertaken using HIER citrate buffer (pH 6.0, ZYTOMED Systems GmbH, Berlin, Germany) in a decloaking chamber (Biocare Medical, Concord, CA). Sections were then blocked using Rodent Blocking Buffer (Biocare Medical), before being incubated over night at 4°C with a primary antibody against cleaved-caspase3 (1:500, AP21655SU-S, Acris Antibodies GmbH, Herford, Germany). These were then incubated with an alkaline phosphatase-labeled secondary antibody (Biocare Medical) for 1hr at room temperature and then the signal amplified with the chromogen substrate Vulcan fast red (Biocare Medical). Sections were counterstained with hematoxylin (Sigma-Aldrich), dehydrated in xylene and cover slips mounted with Entellan (Merck Millipore, Billerica, MA).

Western blot analysis

20µg of protein was resolved by SDS-PAGE and transferred onto a polyvinylidene difluoride membrane (Bio-Rad, Munich, Germany). The membrane was blocked with 5% non-fat milk and immunoblotted overnight at 4°C with anti-cleaved-caspase3 (AP21655SU-S, Acris Antibodies GmbH, Herford, Germany). Antibody binding was detected with a HRP-conjugated goat anti-Rabbit IgG (ab6721, Abcam, Cambridge, UK) followed by developing with Amersham ECL Prime Reagent (GE Healthcare, Freiburg, Germany). Bands were detected and quantified using the Chemidoc XRS system (Bio-Rad), and normalized to β-actin levels (anti-β-actin-peroxidase conjugated mouse monoclonal antibody, A3854, Sigma-Aldrich, St. Louis, MO).

LA4 cell Apoptosis Assay

The murine ATII-like cell line LA4 (ATCC, Rockville, MD) was maintained in Ham's F12 medium containing $NaHCO_3$ and stable glutamine (Biochrom AG, Berlin, Germany), supplemented with 15% fetal calf serum (Gibco, Life Technologies, Darmstadt, Germany), 100U/ml penicillin-streptomycin (Sigma-Aldrich, St. Louis, MO) and 1% Non-Essential Amino Acids (Biochrom AG) at 37°C in 5% CO_2 atmosphere. Cells were Trypsinized (Trypsin-EDTA Solution 1x, Sigma-Aldrich) and seeded at $6x10^4$ cells per well in 24-well plates. 24hrs later, cells we cultured in serum free maintenance medium containing increasing concentrations (0-1mM) of L-carnitine (Sigma-Aldrich) for a further 24hrs. Apoptosis was induced by treating with either, 0.5U/ml PPE for 6hrs in serum free maintenance medium or pulsed with 500uM H_2O_2 (Sigma-Aldrich) for 1hr followed by 48hrs incubation in full maintenance medium supplemented with increasing concentrations (0-1mM) of L-carnitine (Sigma-Aldrich). Apoptosis levels were analyzed using the Annexin V Apoptosis Detection Kit APC (eBioscience, San Diego, CA) as per the manufactures instructions and the stained cells quantified with a BD FACSCanto II flow cytometer (BD Biosciences, Heidelberg, Germany) and BD FACSDiva software.

Analyzing Superoxide Production

MitoSOX Red (Life Technologies, Darmstadt, Germany) was used to analyze the level of mitochondrial superoxide production in LA4 cells. Briefly, LA4 cells seeded at $2x10^5$ cells per well in 12-well plates were cultured for 24hrs in full maintenance medium. Cells were then cultured for a further 24hrs in serum free maintenance medium containing increasing concentrations (0-1mM) of L-carnitine (Sigma-Aldrich). Cells were pulsed with H_2O_2 for 1hr and then incubated for a further 6hrs in serum free maintenance medium. After which they were stained on the plate with medium containing 5µM MitoSOX Red. Cells

were washed with PBS, trypsinized, and resuspended in PBS + 0.5% BSA for analysis on a BD FACSCanto II flow cytometer (BD Biosciences, Heidelberg, Germany). Superoxide production was measured as mean MitoSOX fluorescence intensity in the PE channel.

Statistical analysis

All data analysis, unless indicated otherwise, was undertaken using GraphPad Prism version 6 (GraphPad Software, La Jolla, CA). Results are presented as mean values ± SD. All experiments that contained more than two groups were analyzed using one-way ANOVA following Bonferroni post testing.

RESULTS

Targeted metabolite screening of serum, BALF and lung from emphysematous mice

Intratracheal instillation of porcine pancreatic enzyme (PPE) in mice is known to cause airspace enlargement with breaks in the alveolar wall compatible with destruction (36), that is comparable to emphysema in COPD patients. Despite PPE being shown to be cleared from the lungs of rodents within 24hrs (37), airspace enlargement continues long after this time (18, 36), indeed we have recently shown emphysema following a single oropharangeal application of PPE to continue progressing out to day 161 (19). Here, figure 1A clearly demonstrates a time dependent enlargement of the airspaces in H&E stained lung sections from PPE-treated mice compared to control animals. Lung function analysis of the same mice revealed a time dependent progression in both increasing lung compliance and total lung capacity (TLC) (0.072±0.0096 ml/cmH_2O vs 0.110±0.0092 ml/cmH_2O, $p<0.0001$ for compliance and 1.01±0.08 ml vs 1.30±0.09 ml, $p<0.0001$ for TLC, of PPE treated mice d28 and d161 post exposure respectively) and a reduction in tissue elastance (10.08±1.75cm H_2O/ml vs 6.86±0.63 cm H_2O/ml, $p<0.01$, for PPE treated mice d28 and d161 post exposure respectively) following a single application of PPE (Figure 1B). Thus further confirming the development of progressive emphysema in mice treated with a single dose of PPE. Differential cell counts of cytospins obtained from the BALF confirmed that at later time points emphysema was progressing independently of inflammation in the PPE treated mice (Figure 1C). Indeed, only at d28 was there a slight increase in the BALF macrophage number of PPE treated mice that had returned to baseline by d56. This model therefore provides a great platform to assess potential changes in the mouse metabolome that are occurring during disease progression.

To assess changes in the mouse metabolome during emphysema development; serum, BALF and homogenized lung tissue taken at d28, d56 and d161 from mice exposed to a single application of PPE and their respective PBS controls were analysed using the Absolute*IDQ*™ p180 Kit (Biocrates Life Sciences) that targets acylcarnitines, amino acids, biogenic amines, glycerophospholipids, sphingolipids and hexose. A heat map representation of the significantly changed metabolites across the different tissue types following the application of PPE, at the three time points examined, is demonstrated in Figure 2A. Immediately apparent, perhaps not unsurprisingly, is the increase in the number of metabolites that change as the disease progresses, especially from d28 to d56, with most metabolites being down regulated. Interestingly, a significantly reduced level in a large number of the phosphatidylcholine family members is observed in both the BALF and lung tissue, particularly in BALF during the progression of emphysema (Figure 2A). As proof of principle, a reduction in phosphatidylcholine (PC) has previously been reported in the BALF of emphysema patients and from airway epithelial cells isolated from mice exposed to cigarette smoke for 8 weeks (38, 39).

In a recent study an inverse association between the level of certain plasma sphingomyelins and emphysema in COPD patients was described (15). Although we saw no significant change in serum sphingomyelin levels in our mouse model of emphysema, a number of sphingomyelins were significantly reduced during the progression of emphysema more local to the lung (figure 2A). In the BALF, palmitoylsphingomyelin (SM C16:0), palmitoleicsphingomyelin (SM C16:1), lignoceroylsphingomyelin (SM C24:0), and nervonicsphingomyelin (SM C24:1) were reduced at all three time points examined as well as stearoylsphingomyelin (SM C18:0) and lignoceroylsphingomyelin (SM C24:0) in lung tissue from d56 onwards (Figure 2A). These results are providing lung specific information on sphingomyelin levels and emphysema progression that was lacking from the patient study.

Furthermore, figure 2A also indicates that the pattern of altered metabolites is very compartment specific, with greater changes detectable locally to the lung in both the homogenized tissue and BALF.

This was confirmed in a two dimensional Partial Least Square (PLS) analysis (40) of all metabolites using samples from all mice adjusted for time effect. The PLS revealed that there were major differences in mean metabolite concentrations between PBS and PPE treated mice mainly in the lung tissue and BALF, as can be seen from the first two PLS components separating the two groups almost perfectly in those two tissues and not to the same extent in serum (Figure 2B). To validate the performance of this classification Receiver Operating Characteristic (ROC) curves were generated from 5-fold cross validation and the area under the curve (AUC) was calculated. Figure 2C depicts the mean ROC curves from 5-fold cross validation for all three tissue types plus a reference curve, with an AUC of 0.5, highlighting how a random assignment to treatment groups would appear. With an AUC of 1.0 lung tissue perfectly separates PPE from PBS treated mice, BALF (AUC of 0.96) also shows a high level of separation between the two treatment groups, while serum shows the least level of separation with an AUC of 0.79 (Figure 2C). Taken together, this data suggests that emphysema progression is associated with a reduction in the global metabolomic profile and that this is compartment specific, with most changes being detectable locally to the lung. Furthermore, we confirm previous findings that phospatidylcholine is reduced in the BALF and extend the previous published observation that demonstrated an inverse association between the level of certain plasma sphingomyelins and emphysema, by extending this finding to the lung tissue and BALF. Thus suggesting the PPE induced murine model of emphysema to be a good model of disease progression for further elucidating the underlying molecular mechanisms.

Lung L-carnitine levels are significantly reduced during emphysema

The PLS analysis revealed the greatest level of separation in the metabolomics profile between the PBS and PPE treated groups to be in the lung tissue. Based on this finding we decided to focus in this study only on changes in the emphysematous metabolome that were local to the lung. In Figure 3A we depict the total concentration of lung metabolites stratified by their family class. There was a significant reduction in the concentration of acylcarnitines and amino acids especially at d56 and d161 post PPE treatment, with biogenic amines and lysophosphatidylcholines also showing a reduction to a lower extent (Figure 3A). In order to examine these changes more closely, we analyzed the lung data as volcano plots of mean fold change vs –log10(p value) of individual metabolites (Figure 3B). This revealed an intriguing target L-carnitine, highlighted with a red circle on the volcano plots. In the lung tissue at d56 post PPE treatment L-carnitine was one of the more significantly regulated metabolites, but by d161 it had become the most significantly regulated metabolite in the lung (Figure 3B). Specifically, the concentration of L-carnitine in the lung tissue at all-time points examined, shows that the reduction in the concentration of total acylcarnitines, was predominantly due to a reduction in the level of free L-carnitine (372.71±38.11μM vs 215.50±30.46μM, $p<0.001$, PBS compared to PPE treated mice at d161) (Figure 3C). Our findings show for the first time that L-carnitine reduction predisposed progression of elastase induced-emphysema development.

L-carnitine protects alveolar epithelial type II cells from apoptosis

The enlarged airspaces and reduced surface area characteristic of emphysema is caused by the destruction and loss of alveolar structures, accompanied by increased levels of apoptosis in alveolar epithelial cells (7, 8). Previous studies in a variety of cell types have reported that L-Carnitine protected against oxidative stress, improved mitochondrial function and inhibited apoptosis development (21-26), and interestingly treatment of the human lung epithelial cell line A549 with L-carnitine reversed amiodarone-induced loss of cellular ATP and mitochondrial membrane depolarization (41). We therefore investigated the protective effects of L-carnitine *in vitro* on PPE induced apoptosis of the murine alveolar epithelial type II like cell line-LA4. We first determined if PPE could induce apoptosis of LA4 cells. Figure 4A highlights a dose dependent increase in the level of apoptosis following 6hrs incubation with increasing concentrations of PPE as determined by flow cytometry of Annexin V and PI stained LA4 cells

(14.17±2.14% vs. 46.80±13.10% AnnexinV^{+ve} PI^{+ve}cells, p<0.001, 0U/ml vs. 1U/ml PPE). Further analysis defined that culturing LA4 cells in the presence of L-carnitine up to concentrations of 1mM for up to 72hrs had no detrimental impact on cell viability as determined by flow cytometry of Annexin V^{-ve} and PI^{-ve} stained cells (Figure 4B). Pre-culturing the LA4 cells with increasing concentrations of L-carnitine for 24hrs subsequently reduced the level of apoptosis detected following 6hrs incubation with 0.5U/ml PPE (Figure 4C). Examining the data closely, we observed an overall increase in live cells (29.78±10.05% vs. 56.30±3.00% AnnexinV^{-ve} PI^{-ve}cells, p<0.01, 0mM vs. 1mM L-carnitine) and a reduction in total apoptotic cells (47.13±12.35% vs. 28.83±2.29% Annexin V^{+ve} cells, p<0.05), but there is a slight increase in early apoptotic cells following pretreatment with 1mM L-carnitine (6.50±2.90% vs. 13.28±2.67% AnnexinV^{+ve} PI^{-ve}cells, p<0.01). This is however offset by a reduction in the number of late apoptotic cells (40.88±9.50% vs. 15.70±2.89%, AnnexinV^{+ve} PI^{+ve}cells, p<0.001, 0mM vs. 1mM L-carnitine).

It has previously been shown that H_2O_2-induced apoptosis of alveolar type II cells proceeds through a mechanism of increased intracellular oxidants, mitochondrial membrane depolarization, cytochrome c release and caspase activation (42). Interestingly, ceramide signaling has also been reported to act as the second messenger in H_2O_2-induced apoptosis of human airway epithelial cells (43), upregulation of ceramide has been associated with pulmonary cell apoptosis in emphysema (44). We therefore examined the ability of L-carnitine to inhibit H_2O_2-induced apoptosis of LA4 cells. LA4 cells were cultured in the presence of increasing concentrations of L-carnitine for 24hrs, pulsed for 1hr with 500µM H_2O_2 and then cultured for a further 48hrs with L-carnitine. Figure 5A clearly shows a dose dependent reduction in the number of both early (25.55±3.41% vs. 8.48±3.60% AnnexinV^{+ve} PI^{-ve}cells, p<0.0001, 0mM vs. 1mM L-carnitine) and late (54.10±3.27 vs. 23.58±11.04 AnnexinV^{+ve} PI^{+ve}cells, p<0.001, 0mM vs. 1mM L-carnitine) apoptotic LA4 cells, with a concomitant increase in live cells, when cultured in the presence of elevated concentrations of L-carnitine. To assess levels of mitochondrial superoxide, as a marker of reactive oxygen species production, we stained LA4 cells with the mitochondria-specific probe MitoSOX Red. Staining with MitoSOX Red revealed that L-carnitine protection against H_2O_2-induced apoptosis was accompanied by reduced generation of mitochondrial superoxide (Figure 5B), in keeping with the proposed anti-oxidant function of L-carnitine. Interestingly, culturing LA4 cells in the presence of L-carnitine without H_2O_2 treatment also significantly reduced the level of mitochondrial superoxide, but only at the highest dose examined.

Taken together these results demonstrate that PPE, a strong inducer of progressive emphysema *in vivo*, can induce apoptosis of ATII like cells *in vitro* and for the first time we show that L-carnitine can provide protection against PPE induced apoptosis of ATII cells. Furthermore, we confirmed an anti-oxidant role for L-carnitine in protecting ATII cells against H_2O_2-induced apoptosis.

L-carnitine attenuates emphysema development

Our metabolomics screen identified L-carnitine to be one of the most significantly reduced metabolites in the lung during the progression of PPE induced emphysema. This, along with its protective function against PPE-induced apoptosis of LA4 cells described above, prompted us to examine if supplementation of mice with L-carnitine could attenuate the development of PPE induced emphysema. Mice were supplemented every second day i.p. with L-carnitine at a dose of 500mg/kg body weight (28, 45) following a single oropharyngeal administration of PPE. Figure 6A highlights that systemic application of L-carnitine results in a significant increase in the concentration of lung specific L-carnitine at d28 compared to animals only administered PPE, and that this was approaching levels detected in PBS treated control mice. Differential cell counts of cytospins obtained from the BALF confirmed that by d28 emphysema was progressing independently of inflammation in PPE treated mice (Figure 6B). Interestingly, western blot analysis of lung homogenate revealed increased levels of active cleaved-

caspase 3, the executioner of apoptosis (46), in mice treated with PPE compared to control PBS, and that this was reduced following supplementation with L-carnitine (Figure 6C). Furthermore, morphological analysis of tissue sections stained for cleaved-caspase 3 demonstrated the presence of apoptotic alveolar epithelial cells, airway epithelial cells and endothelial cells within the lung of emphysematous mice induced by PPE (Figure 6D). The presence of apoptotic alveolar epithelial cells was drastically reduced following L-carnitine supplementation, as confirmed by quantification using the newCAST system ($p<0.01$, Figure 6D), but some apoptotic endothelial and airway epithelial cells could still be detected in the supplemented group albeit to a lesser extent than in PPE only treated mice.

Finally, we analyzed physiological and pathological parameters in the above emphysematous mice. We observed an improved lung function following L-carnitine supplementation (Figure 7A). PPE-treated animals had increased lung compliance (0.067 ± 0.008 ml/cmH_20 vs 0.035 ± 0.005 ml/cmH_20, $p<0.0001$) compared to PBS-treated controls, which improved following supplementation with L-carnitine 0.051 ± 0.006 ml/cmH_20, $p<0.01$ compared to mice only treated with PPE. This was accompanied by a concomitant increase ($p<0.05$) in lung elastance of L-carnitine supplemented PPE-treated mice compared to their PPE-treated counterparts (Figure 7A). Furthermore, the increase in TLC observed in PPE-treated mice compared to PBS-treated controls (0.93 ± 0.11 vs 0.63 ± 0.08, $p<0.001$), was slightly reduced following L-carnitine supplementation (0.81 ± 0.07) but did not reach statistical significance when compared to PPE-treated mice (Figure 7A). Surprisingly, despite a clear demonstration of enlargement of the airspaces in H&E stained lung sections from PPE-treated mice compared to control animals, consistent with their poor lung function, we did not observe an improved airspace enlargement to accompany the improved lung function observed in the L-carnitine supplemented mice (Figure 7B). Taken together, L-carnitine supplementation protects against the alveolar cell apoptosis that accompanies emphysema progression and improves lung function in PPE-induced emphysematous mice.

DISCUSSION

This study used mass spectrometry–based targeted metabolomics followed by systems biological approaches to quantitate the lung tissue, BALF and serum metabolome at three different time points during emphysema progression in the PPE-induced murine model, to further elucidate mechanisms of progression in emphysema development. We demonstrate that changes in the metabolome are compartment specific, with a greater change being detected local to the lung rather than the serum, and for the first time reported that emphysema progression is accompanied by a reduction in lung-specific L-carnitine. Furthermore, supplementation with L-carnitine impaired apoptosis of alveolar cells both *in vitro* and *in vivo*, and this was accompanied by an improvement in lung function of PPE-induced emphysematous mice.

Metabolomics is a powerful tool that can reveal a greater depth of understanding about the biochemical pathways of cells, thus providing a detailed profiling of the physiological changes in tissues and organisms during steady state and disease progression than simply gene expression, to potentially reveal new underlying pathophysiological mechanisms and biomarkers of disease progression. This is substantiated by the rapid increase in studies over the last 5 years assessing metabolomic changes in COPD patients and animal models of disease (10-17). These studies however, lack a thorough analysis of metabolomic changes occurring in the lung tissue during the progression of emphysema. This may not be the ideal tissue for a biomarker given the difficulties in obtaining biopsies from patients, but is critical in furthering our understanding of the mechanisms of disease progression. To that end we chose to assess the well-established PPE-induced murine model of emphysema, as it induces airspace enlargement similar to that observed in COPD patients (36), a single treatment leads to progressive disease that is associated with senescence of alveolar epithelial cells (19) and accompanied by increased levels of apoptosis (47). In this study we confirm that a single oropharyngeal application of PPE resulted in a progressive emphysematous phenotype out to day 161, which is associated with a steady decline in lung function and an increase in lung volume that accompanies an increase in airspace enlargement. We also demonstrate that PPE-induced emphysema is accompanied by increased levels of apoptosis in alveolar epithelial cells, airway epithelial cells and endothelial cells.

Pulmonary surfactant secreted by alveolar epithelial type II cells to reduce pulmonary surface tension at the air-liquid-interface of alveolar spaces is composed of key surfactant proteins and several classes of lipid, with 80% of surfactant lipid comprising of phosphatidylcholine (PC) (48). Ridsdale et al. demonstrated that the BALF of emphysematous patients contained less PC 16:0/14:0 compared to controls (38), and a study examining airway epithelial cells isolated from mice exposed to cigarette smoke for 8 weeks reported a decrease of 61% in the level of total PC compared to filtered air controls (39). Our analysis of altered metabolites clearly demonstrates from d56 onwards a significant reduction of PC family members in both the lung tissue sample and BALF. Indeed, over 40 PC family members of both diacylPC and acyl-alkylPC species were significantly reduced in the BALF at d56 and d161, including PC C30:0 the same lipid as described in the patient study. Two other major PC components of pulmonary surfactant PC 16:0/16:0 and PC 16:0/16:1 (49) were also significantly reduced in the BALF of PPE-exposed mice at d56 and d161 compared to PBS controls. It is interesting to highlight that L-carnitine has been reported to be important for the production of pulmonary surfactant PC in the fetal lung. Treatment of pregnant rats with L-carnitine resulted in significant increases in the amounts of both total phospholipid and PC 16:0/16:0 in fetal rat lung, which was accompanied by increased numbers of lamellar bodies in type II cell progenitors (50). Our metabolic screen revealed significant reduction in the levels of lung L-carnitine, including free L-carnitine (C0) and L-carnitine C16 (L-carnitine is attached to the same length fatty acid chain that is found attached to the predominant PCs of pulmonary surfactant)

from d56 onwards, which coincides with the reduction in BALF PC. One could therefore speculate that the reduction observed in PC is the result of lowered levels of L-carnitine in the emphysematous lung during disease progression.

We also demonstrated that the emphysematous lung and BALF compared to control mice contained reduced levels of sphingomyelin lipids with both long-chain and very long-chain fatty acids attached. A very recent study of COPD patients, using both targeted and untargeted metabolic approaches, revealed an inverse association between the level of some plasma sphingomyelins and emphysema severity (15). Of the 5 sphingomyelins validated by both screens in that study, 4 were also reduced in our study and the 5th sphingomyelin C14:0 was not detected by our kit. We did not detect any significant changes in the levels of serum sphingomyelin in contrast to the patient study. However, another group assessing the level of plasma sphingomyelin in 3840 participants and measuring pulmonary emphysema using computed tomography reported higher plasma levels of sphingomyelin was associated with increased progression of emphysema (51).

Our most interesting observation is that the progression of emphysema is associated with a reduction in the levels of lung L-carnitine, in fact by day 161 L-carnitine had become the most significantly altered metabolite in the lung. Interestingly, Elsammak and colleagues previously demonstrated a significant reduction in plasma total and free carnitine levels in COPD patients compared to healthy controls, which significantly correlated with severe (FEV1 ≥ 30% to < 50% predicted) and very severe (FEV1 < 30%) patients only (52). The primary function of L-carnitine is to transport long-chain fatty acids into the mitochondrial matrix for their subsequent beta-oxidation and energy production via the tricarboxylic acid cycle (20). Long-chain fatty acids are first activated by the enzyme long-chain acyl-CoA synthetase in the mitochondrial outer membrane to form acyl-CoAs, which cannot enter the mitochondrial matrix. They are therefore catalyzed by another mitochondrial outer membrane enzyme, carnitine palmitoyltransferase I, which replaces CoA with L-carnitine, to form the long-chain acylcarnitines. These are then transported into the mitochondrial matrix via the integral mitochondrial inner membrane protein carnitine:acylcarnitine translocase (CACT). The importance of L-carnitine is highlighted by neonates that suffer primary systemic carnitine deficiency due to mutations in the gene encoding OCTN2 (53), because of reduced beta-oxidation energy production is down which particularly affects skeletal and cardiac muscles presenting as myopathy, if left unchecked it can progress to a systemic syndrome of hypotonia, hypoglycemia, hypoketonia, encephalopathy, coma and perhaps death, however patients respond very well to L-carnitine supplementation (30). In addition to its role in the oxidation of fatty acids, L-carnitines ability to accept fatty acid chains from acyl-CoA, means it is important in regulating the ratio of free CoA to acyl-CoA. A reduction in the levels of L-carnitine results in a reduction in mitochondrial free CoA and increased acyl-CoA which inhibits the function of several mitochondrial dehydrogenases impairing carbohydrate utilization, amino acid catabolism and the detoxification of xenobiotics (54). A lung with such disrupted metabolic homeostasis is unlikely to have a balance in favor of repair and regeneration over injury.

In contrast to the deleterious effects of reduced L-carnitine, we have shown here that apoptosis induced in the ATII like cell line LA4 by both PPE and H_2O_2 can be prevented by pretreating the cells with L-carnitine. It has been suggested that PPE-treated lung epithelial cells upregulate placenta growth factor which induces apoptosis via signaling through the JNK and p38 MAPK pathways (47). Signaling through these kinases can result in the mitochondrial mediated (intrinsic) apoptotic pathway - translocation of Bax and Bim to the mitochondria, followed by cytochrome c release and caspase activation (55, 56). Mitochondrial permeability transition is key for cytochrome c release (57), and it is interesting to note that L-carnitine has been shown to inhibit the mitochondrial permeability transition on isolated rat liver

mitochondria (58). Furthermore, it has been demonstrated *in vitro* that L-carnitine has the ability to directly inhibit the proteolytic activity of both an initiator and effector caspase, caspases 8 and 3 respectively (25). Conventionally, one thinks of H_2O_2-induced apoptosis to progress through a mechanism of increased intracellular oxidants, mitochondrial membrane polarization, cytochrome c release and caspase activation, as has been described for type II cells (42). We demonstrate that pre-treatment of LA4 cells with L-carnitine reduces the amount of mitochondrial superoxide production following H_2O_2 treatment, which may offer another potential anti-apoptotic mode of action for L-carnitine, as has also been suggested following H_2O_2 treatment of the human proximal tubule epithelial cell line, HK-2 (21). More intriguing is the mechanism of action demonstrated in cardiac myocytes, that L-carnitine can block the increase in intracellular ceramide levels by inhibiting the action of acid sphingomyelinase (22). Interestingly, upregulation of ceramide has been shown to precede caspase-3 activation during apoptosis of A549 cells (59), although the increases in ceramide following H_2O_2 treatment of human airway epithelial cells is via the action of neutral sphingomyelinase (43). Increases in the levels of ceramide have also been associated with pulmonary cell apoptosis in animal models of emphysema, and in the same study increased ceramide was also observed in the alveolar septal cells of emphysematous patients (44).

The benefit to mitochondrial homeostasis described following L-carnitine supplementation and the positive effects on inhibiting apoptosis *in vitro* led us to hypothesize that supplementing with L-carnitine would attenuate the development of emphysema in PPE-treated mice. Supplementing mice i.p. with L-carnitine increased the level of lung L-carnitine following PPE-treatment which was accompanied by a significant improvement in lung function and in the level of apoptosis. The caveat to this is that there did not appear to be any improvement to the air space enlargement compared to PPE treatment alone. One potential reason for this and critique of the study was the time of analysis following supplementation. We assessed the lungs 28 days post instillation to examine if L-carnitine supplementation early could slow the progression of emphysema, however it is possible that L-carnitine is more important for disease progression rather than initiation. Additionally, the route of delivery for L-carnitine can also be discussed in this context. The lung as an organ manifests perfectly for local drug delivery, but we used i.p. application. Aside from ease of administration, an *in vivo* study in mice using the ovalbumin model of asthma reported that i.p. delivery of L-carnitine improved oxygen saturation and improved bronchial associated inflammation (28), additionally administration of L-carnitine in the drinking water of rats reduced the level of lipid peroxide found in the lung following bleomycin treatment (45). In our study, following i.p. administration of L-carnitine, L-carnitine levels in the lung were greater than PPE-treated mice alone, which was accompanied by an improvement in lung function and apoptosis. IHC of lung sections for activated caspase 3 revealed that apoptotic alveolar epithelial type II cells were reduced following L-carnitine supplementation but some apoptotic endothelial and airway epithelial cells could still be detected in the supplemented group. The remaining apoptotic cells in the lungs of our supplemented mice may thus be preventing a balance in favor of regeneration and therefore comparable airspace enlargement is observed across the two groups. Sufficient blocking of apoptosis by inhibiting the MAP kinase pathways or using siRNA knock down of placenta growth factor inhibited airspace enlargement following PPE-exposure (47).

To expand upon our findings presented here, we further plan to assess the beneficial effects of L-carnitine supplementation during chronic cigarette smoke exposure, a model of COPD in which emphysema is accompanied by chronic inflammation and airway remodeling (32, 60). It has been known for some time that oxidative stress following cigarette smoking is involved in many of the pathological processes underlying COPD (61) and more recently cigarette smoke has been shown to impair mitochondrial function (62). L-carnitines established role as an antioxidant and enhancer of

mitochondrial function (21, 23, 24) would thus lend it to having additional beneficial effects against chronic cigarette smoke induced lung injury.

In summary, targeted metabolomics reveals for the first time that the progression of emphysema is accompanied by a reduction in the lungs of the metabolite L-carnitine. L-carnitine supplementation impaired apoptosis of alveolar cells both *in vitro* and *in vivo*, and this was accompanied by an improvement in lung function of PPE-induced emphysematous mice. We would therefore like to suggest that L-carnitine supplementation of COPD patients in parallel with their current treatment regime could slow or even regress disease progression.

Clinical Perspective

It is not clear what drives disease progression in emphysematous patients, indeed progression amongst individuals is highly variable. Therefore, we performed a targeted metabolomics approach to identify novel metabolic pathways in a clinically relevant progressive emphysema mouse model, to highlight new targets and biomarkers that may be key in furthering our understanding of disease progression.

We demonstrate that changes to the metabolome were very compartmentalized with greater changes detectable in the lung tissue and BALF rather than the serum. Furthermore, this study shows for the first time, that emphysema progression is associated with a reduction in lung tissue specific L-carnitine, a critical metabolite with anti-oxidant and anti-apoptotic properties. Additionally, supplementing mice with this metabolite impeded disease progression.

The identification of metabolomic changes local to the injured tissue are key in identifying good biomarkers for disease progression and critical in furthering our understanding of the mechanisms of disease progression and for identifying novel therapeutic targets.

Acknowledgements
The authors acknowledge the help of Christine Hollauer and Joanna Schmucker. We thank Julia Scarpa, Werner Römisch-Margl and Katharina Faschinger for metabolomics measurements performed at the Helmholtz Zentrum München, Genome Analysis Center, Metabolomics Core Facility.

Declarations of interest
The authors declare they have no conflict of interest.

Funding Information
This work was supported in part by the Helmholtz Association, The German Center for Lung Research (DZL) and a grant from the German Federal Ministry of Education and Research (BMBF) to the German Center Diabetes Research (DZD e.V.).

Author contributions
TMC, KB, CP, JA, OE & AÖY designed experiments; TMC, KB & CP conducted experiments; JB, JK & FJT designed and undertook data analysis of metabolomics data; TMC & AÖJ wrote the manuscript; all authors contributed to scientific discussions and read the manuscript.

References

1. Pauwels RA, Buist AS, Calverley PM, Jenkins CR, Hurd SS, Committee GS. Global strategy for the diagnosis, management, and prevention of chronic obstructive pulmonary disease. NHLBI/WHO Global Initiative for Chronic Obstructive Lung Disease (GOLD) Workshop summary. American journal of respiratory and critical care medicine. 2001;163(5):1256-76.
2. McDonough JE, Yuan R, Suzuki M, Seyednejad N, Elliott WM, Sanchez PG, et al. Small-airway obstruction and emphysema in chronic obstructive pulmonary disease. The New England journal of medicine. 2011;365(17):1567-75.
3. Hautamaki RD, Kobayashi DK, Senior RM, Shapiro SD. Requirement for macrophage elastase for cigarette smoke-induced emphysema in mice. Science. 1997;277(5334):2002-4.
4. Wiedemann HP, Stoller JK. Lung disease due to alpha 1-antitrypsin deficiency. Current opinion in pulmonary medicine. 1996;2(2):155-60.
5. Kanazawa H, Yoshikawa J. Elevated oxidative stress and reciprocal reduction of vascular endothelial growth factor levels with severity of COPD. Chest. 2005;128(5):3191-7.
6. Tsuji T, Aoshiba K, Nagai A. Alveolar cell senescence in patients with pulmonary emphysema. American journal of respiratory and critical care medicine. 2006;174(8):886-93.
7. Kasahara Y, Tuder RM, Cool CD, Lynch DA, Flores SC, Voelkel NF. Endothelial cell death and decreased expression of vascular endothelial growth factor and vascular endothelial growth factor receptor 2 in emphysema. American journal of respiratory and critical care medicine. 2001;163(3 Pt 1):737-44.
8. Calabrese F, Giacometti C, Beghe B, Rea F, Loy M, Zuin R, et al. Marked alveolar apoptosis/proliferation imbalance in end-stage emphysema. Respiratory research. 2005;6:14.
9. Mittelstrass K, Ried JS, Yu Z, Krumsiek J, Gieger C, Prehn C, et al. Discovery of sexual dimorphisms in metabolic and genetic biomarkers. PLoS genetics. 2011;7(8):e1002215.
10. Deja S, Porebska I, Kowal A, Zabek A, Barg W, Pawelczyk K, et al. Metabolomics provide new insights on lung cancer staging and discrimination from chronic obstructive pulmonary disease. Journal of pharmaceutical and biomedical analysis. 2014;100:369-80.
11. Wang L, Tang Y, Liu S, Mao S, Ling Y, Liu D, et al. Metabonomic profiling of serum and urine by (1)H NMR-based spectroscopy discriminates patients with chronic obstructive pulmonary disease and healthy individuals. PloS one. 2013;8(6):e65675.
12. Paige M, Burdick MD, Kim S, Xu J, Lee JK, Shim YM. Pilot analysis of the plasma metabolite profiles associated with emphysematous Chronic Obstructive Pulmonary Disease phenotype. Biochemical and biophysical research communications. 2011;413(4):588-93.
13. Telenga ED, Hoffmann RF, Ruben tK, Hoonhorst SJ, Willemse BW, van Oosterhout AJ, et al. Untargeted lipidomic analysis in chronic obstructive pulmonary disease. Uncovering sphingolipids. American journal of respiratory and critical care medicine. 2014;190(2):155-64.
14. Ubhi BK, Cheng KK, Dong J, Janowitz T, Jodrell D, Tal-Singer R, et al. Targeted metabolomics identifies perturbations in amino acid metabolism that sub-classify patients with COPD. Molecular bioSystems. 2012;8(12):3125-33.
15. Bowler RP, Jacobson S, Cruickshank C, Hughes GJ, Siska C, Ory DS, et al. Plasma sphingolipids associated with chronic obstructive pulmonary disease phenotypes. American journal of respiratory and critical care medicine. 2015;191(3):275-84.
16. Cruickshank-Quinn CI, Mahaffey S, Justice MJ, Hughes G, Armstrong M, Bowler RP, et al. Transient and persistent metabolomic changes in plasma following chronic cigarette smoke exposure in a mouse model. PloS one. 2014;9(7):e101855.

17. Li J, Yang L, Li Y, Tian Y, Li S, Jiang S, et al. Metabolomics study on model rats of chronic obstructive pulmonary disease treated with BuFei JianPi. Molecular medicine reports. 2015;11(2):1324-33.
18. Yildirim AO, Muyal V, John G, Muller B, Seifart C, Kasper M, et al. Palifermin induces alveolar maintenance programs in emphysematous mice. American journal of respiratory and critical care medicine. 2010;181(7):705-17.
19. Sarker RS, John-Schuster G, Bohla A, Mutze K, Burgstaller G, Bedford MT, et al. CARM1 Regulates Alveolar Epithelial Senescence and Elastase-induced Emphysema Susceptibility. American journal of respiratory cell and molecular biology. 2015.
20. Kerner J, Hoppel C. Fatty acid import into mitochondria. Biochimica et biophysica acta. 2000;1486(1):1-17.
21. Ye J, Li J, Yu Y, Wei Q, Deng W, Yu L. L-carnitine attenuates oxidant injury in HK-2 cells via ROS-mitochondria pathway. Regulatory peptides. 2010;161(1-3):58-66.
22. Andrieu-Abadie N, Jaffrezou JP, Hatem S, Laurent G, Levade T, Mercadier JJ. L-carnitine prevents doxorubicin-induced apoptosis of cardiac myocytes: role of inhibition of ceramide generation. FASEB journal : official publication of the Federation of American Societies for Experimental Biology. 1999;13(12):1501-10.
23. Calo LA, Pagnin E, Davis PA, Semplicini A, Nicolai R, Calvani M, et al. Antioxidant effect of L-carnitine and its short chain esters: relevance for the protection from oxidative stress related cardiovascular damage. International journal of cardiology. 2006;107(1):54-60.
24. Geier DA, Geier MR. L-carnitine exposure and mitochondrial function in human neuronal cells. Neurochemical research. 2013;38(11):2336-41.
25. Mutomba MC, Yuan H, Konyavko M, Adachi S, Yokoyama CB, Esser V, et al. Regulation of the activity of caspases by L-carnitine and palmitoylcarnitine. FEBS letters. 2000;478(1-2):19-25.
26. Vescovo G, Ravara B, Gobbo V, Sandri M, Angelini A, Della Barbera M, et al. L-Carnitine: a potential treatment for blocking apoptosis and preventing skeletal muscle myopathy in heart failure. American journal of physiology Cell physiology. 2002;283(3):C802-10.
27. Al-Biltagi M, Isa M, Bediwy AS, Helaly N, El Lebedy DD. L-carnitine improves the asthma control in children with moderate persistent asthma. Journal of allergy. 2012;2012:509730.
28. Uzuner N, Kavukcu S, Yilmaz O, Ozkal S, Islekel H, Karaman O, et al. The role of L-carnitine in treatment of a murine model of asthma. Acta medica Okayama. 2002;56(6):295-301.
29. Borghi-Silva A, Baldissera V, Sampaio LM, Pires-DiLorenzo VA, Jamami M, Demonte A, et al. L-carnitine as an ergogenic aid for patients with chronic obstructive pulmonary disease submitted to whole-body and respiratory muscle training programs. Brazilian journal of medical and biological research = Revista brasileira de pesquisas medicas e biologicas / Sociedade Brasileira de Biofisica [et al]. 2006;39(4):465-74.
30. Crill CM, Helms RA. The use of carnitine in pediatric nutrition. Nutrition in clinical practice : official publication of the American Society for Parenteral and Enteral Nutrition. 2007;22(2):204-13.
31. John G, Kohse K, Orasche J, Reda A, Schnelle-Kreis J, Zimmermann R, et al. The composition of cigarette smoke determines inflammatory cell recruitment to the lung in COPD mouse models. Clinical science. 2014;126(3):207-21.
32. John-Schuster G, Hager K, Conlon TM, Irmler M, Beckers J, Eickelberg O, et al. Cigarette smoke-induced iBALT mediates macrophage activation in a B cell-dependent manner in COPD. American journal of physiology Lung cellular and molecular physiology. 2014;307(9):L692-706.
33. Romisch-Margl W, Prehn C, Bogumil R, Rohring C, Suhre K, Adamski J. Procedure for tissue sample preparation and metabolite extraction for high-throughput targeted metabolomics. Metabolomics. 2012;8(1):133-42.

34. Zukunft S, Sorgenfrei M, Prehn C, Moller G, Adamski J. Targeted Metabolomics of Dried Blood Spot Extracts. Chromatographia. 2013;76(19-20):1295-305.
35. Li HD, Xu QS, Liang YZ. libPLS: An integrated Library for Partial Least Squares Regression and Discriminant Analysis. PeerJ PrePrints. 2014;2:e190v1.
36. Lucey EC, Keane J, Kuang PP, Snider GL, Goldstein RH. Severity of elastase-induced emphysema is decreased in tumor necrosis factor-alpha and interleukin-1beta receptor-deficient mice. Laboratory investigation; a journal of technical methods and pathology. 2002;82(1):79-85.
37. Stone PJ, Lucey EC, Calore JD, McMahon MP, Snider GL, Franzblau C. Defenses of the hamster lung against human neutrophil and porcine pancreatic elastase. Respiration; international review of thoracic diseases. 1988;54(1):1-15.
38. Ridsdale R, Roth-Kleiner M, D'Ovidio F, Unger S, Yi M, Keshavjee S, et al. Surfactant palmitoylmyristoylphosphatidylcholine is a marker for alveolar size during disease. American journal of respiratory and critical care medicine. 2005;172(2):225-32.
39. Agarwal AR, Yin F, Cadenas E. Short-term cigarette smoke exposure leads to metabolic alterations in lung alveolar cells. American journal of respiratory cell and molecular biology. 2014;51(2):284-93.
40. Lorber A, Wangen LE, Kowalski BR. A theoretical foundation for the PLS algorithm Journal of Chemometrics. 1987;1(1):19-31.
41. Yano T, Itoh Y, Yamada M, Egashira N, Oishi R. Combined treatment with L-carnitine and a pan-caspase inhibitor effectively reverses amiodarone-induced injury in cultured human lung epithelial cells. Apoptosis : an international journal on programmed cell death. 2008;13(4):543-52.
42. Yin L, Stearns R, Gonzalez-Flecha B. Lysosomal and mitochondrial pathways in H2O2-induced apoptosis of alveolar type II cells. Journal of cellular biochemistry. 2005;94(3):433-45.
43. Castillo SS, Levy M, Thaikoottathil JV, Goldkorn T. Reactive nitrogen and oxygen species activate different sphingomyelinases to induce apoptosis in airway epithelial cells. Experimental cell research. 2007;313(12):2680-6.
44. Petrache I, Natarajan V, Zhen L, Medler TR, Richter AT, Cho C, et al. Ceramide upregulation causes pulmonary cell apoptosis and emphysema-like disease in mice. Nature medicine. 2005;11(5):491-8.
45. Daba MH, Abdel-Aziz AA, Moustafa AM, Al-Majed AA, Al-Shabanah OA, El-Kashef HA. Effects of L-carnitine and ginkgo biloba extract (EG b 761) in experimental bleomycin-induced lung fibrosis. Pharmacological research : the official journal of the Italian Pharmacological Society. 2002;45(6):461-7.
46. Budihardjo I, Oliver H, Lutter M, Luo X, Wang X. Biochemical pathways of caspase activation during apoptosis. Annual review of cell and developmental biology. 1999;15:269-90.
47. Hou HH, Cheng SL, Liu HT, Yang FZ, Wang HC, Yu CJ. Elastase induced lung epithelial cell apoptosis and emphysema through placenta growth factor. Cell death & disease. 2013;4:e793.
48. Agassandian M, Mallampalli RK. Surfactant phospholipid metabolism. Biochimica et biophysica acta. 2013;1831(3):612-25.
49. Bernhard W, Hoffmann S, Dombrowsky H, Rau GA, Kamlage A, Kappler M, et al. Phosphatidylcholine molecular species in lung surfactant: composition in relation to respiratory rate and lung development. American journal of respiratory cell and molecular biology. 2001;25(6):725-31.
50. Lohninger A, Bock P, Dadak C, Feiks A, Kaiser E. Effect of carnitine on foetal rat lung dipalmitoyl phosphatidylcholine content and lung morphology. Carnitine and lung surfactant, I. Journal of clinical chemistry and clinical biochemistry Zeitschrift fur klinische Chemie und klinische Biochemie. 1990;28(5):313-8.
51. Ahmed FS, Jiang XC, Schwartz JE, Hoffman EA, Yeboah J, Shea S, et al. Plasma sphingomyelin and longitudinal change in percent emphysema on CT. The MESA lung study. Biomarkers : biochemical indicators of exposure, response, and susceptibility to chemicals. 2014;19(3):207-13.

52. Elsammak MMY, Attia A, Suleman M. Carnitine Deficiency in Chronic Obstructive Pulmonary Disease Patients. J Pulmonar Respirat Med. 2011;1:106.
53. Nezu J, Tamai I, Oku A, Ohashi R, Yabuuchi H, Hashimoto N, et al. Primary systemic carnitine deficiency is caused by mutations in a gene encoding sodium ion-dependent carnitine transporter. Nature genetics. 1999;21(1):91-4.
54. Marcovina SM, Sirtori C, Peracino A, Gheorghiade M, Borum P, Remuzzi G, et al. Translating the basic knowledge of mitochondrial functions to metabolic therapy: role of L-carnitine. Translational research : the journal of laboratory and clinical medicine. 2013;161(2):73-84.
55. Kurinna SM, Tsao CC, Nica AF, Jiffar T, Ruvolo PP. Ceramide promotes apoptosis in lung cancer-derived A549 cells by a mechanism involving c-Jun NH2-terminal kinase. Cancer research. 2004;64(21):7852-6.
56. Van Laethem A, Van Kelst S, Lippens S, Declercq W, Vandenabeele P, Janssens S, et al. Activation of p38 MAPK is required for Bax translocation to mitochondria, cytochrome c release and apoptosis induced by UVB irradiation in human keratinocytes. FASEB journal : official publication of the Federation of American Societies for Experimental Biology. 2004;18(15):1946-8.
57. Narita M, Shimizu S, Ito T, Chittenden T, Lutz RJ, Matsuda H, et al. Bax interacts with the permeability transition pore to induce permeability transition and cytochrome c release in isolated mitochondria. Proceedings of the National Academy of Sciences of the United States of America. 1998;95(25):14681-6.
58. Pastorino JG, Snyder JW, Serroni A, Hoek JB, Farber JL. Cyclosporin and carnitine prevent the anoxic death of cultured hepatocytes by inhibiting the mitochondrial permeability transition. The Journal of biological chemistry. 1993;268(19):13791-8.
59. Ravid T, Tsaba A, Gee P, Rasooly R, Medina EA, Goldkorn T. Ceramide accumulation precedes caspase-3 activation during apoptosis of A549 human lung adenocarcinoma cells. American journal of physiology Lung cellular and molecular physiology. 2003;284(6):L1082-92.
60. John-Schuster G, Günter S, Hager K, Conlon TM, Eickelberg O, Yildirim AÖ. Inflammaging increases susceptibility to cigarette smoke-induced COPD. Oncotarget. 2015;Advance Publications.
61. MacNee W. Oxidants and COPD. Current drug targets Inflammation and allergy. 2005;4(6):627-41.
62. Ballweg K, Mutze K, Konigshoff M, Eickelberg O, Meiners S. Cigarette smoke extract affects mitochondrial function in alveolar epithelial cells. American journal of physiology Lung cellular and molecular physiology. 2014;307(11):L895-907.

FIGURE LEGENDS

Figure 1. A single oropharyngeal application of porcine pancreatic elastase (PPE) leads to the development of a progressive emphysema in the lungs of mice. A: Representative photomicrographs of H&E stained lung sections from PBS and PPE-treated mice at the time points indicated. Scale bar 200µm. Airspace enlargement was quantified as the mean linear intercept (MLI) by design-based stereology using the newCAST system. **B:** Lung function measurements to obtain total lung capacity, tissue elastance and dynamic compliance in PBS and PPE-treated mice at the time points indicated. **C:** Total and differential cell counts in the BALF. Data shown are from one experiment with 6-11 mice per group at each time point, with mean values ± SD given. One-way ANOVA following Bonferroni post test with $*P < 0.05$, $**P < 0.01$, $***P < 0.001$, $****P < 0.0001$.

Figure 2. Targeted metabolomics reveals that there are greater changes in the metabolome local to the lung than in the serum during the progression of PPE-induced emphysema. Metabolomics screening using the Absolute*IDQ*™ p180 Kit followed by mass spectrometric analysis of serum, BALF and lung homogenate was undertaken on the mice described in Figure 1. **A:** Heat maps demonstrating the mean relative fold change in individual metabolite concentrations in mice exposed to PPE compared to PBS controls at the time points indicated. A white box means the metabolite was not significantly altered in that tissue at that time point ($P > 0.05$, t-test) following univariate analysis. A blue box represents an increase in the metabolite and yellow a decrease. **B:** Two dimensional partial least square analyses of all metabolites in all mice at every time point. Each dot represents an individual mouse. LV, latent variable. **C:** Receiver operating characteristics (ROC) curve generated from 5 fold cross validation of the PLS analysis. A representative model for each tissue type is shown plus a reference curve, along with the area under the curve (AUC).

Figure 3. L-carnitine is the most significantly altered lung metabolite during emphysema progression. A: The sum total in the concentration of lung tissue metabolites detected within the class indicated, at the time points shown. **B:** A plot of the mean $\log_2$(relative fold change) versus $-\log_{10}(P)$ for each individual metabolite at the time point indicated in lung tissue, from PPE-treated mice compared to PBS controls. Significance was taken as $P < 0.05$ (t-test) and a fold change > 0.3 in either direction, as indicated by the red data points and hatched lines. Free L-carnitine (C0) is highlighted by a red circle. **C:** The concentration of free L-carnitine (C0) in lung tissue. Data shown is the mean value ± SD from 6-11 mice per group at each time point taken from the Absolute*IDQ*™ p180 metabolomics screen, with $*P < 0.05$, $**P < 0.01$, $***P < 0.001$, $****P < 0.0001$ following t-test.

Figure 4. Pre-treatment with L-carnitine protects LA4 cells from PPE-induced apoptosis. A: The ATII like cell line LA4 was cultured with increasing concentrations of PPE for 6hr and then the level of apoptosis determined by staining with Annexin V and PI, followed by flow cytometric analysis. Representative facs plots are demonstrated, with mean quadrant values indicated. Data shown is the percentage of cells (mean ± SD) from the following quadrants - Live Cells, Annexin V^{-ve} PI^{-ve}; Total Apoptptic, all Annexin V^{+ve} cells; Early Apoptotic, Annexin V^{+ve} PI^{-ve}; Late Apoptotic, Annexin V^{+ve} PI^{+ve}. **B:** LA4 cells were cultured with increasing concentrations of L-carnitine for the time points shown and viability determined as in A. **C:** LA4 cells were cultured for 24hrs in the presence of L-carnitine at the concentrations shown followed by 6hrs incubation with PPE at a concentration of 0.5U/ml. The level of apoptosis was determined as in A. For all charts mean values ± SD from one representative experiment (n=3-4) repeated two to three times is shown. One-way ANOVA following Bonferroni post test was undertaken with $*P < 0.05$, $**P < 0.01$, $***P < 0.001$, $****P < 0.0001$ compared to the control group.

Figure 5. H_2O_2 induced apoptosis of LA4 cells is prevented by pre-treatment with L-carnitine. **A:** LA4 cells were cultured for 24hrs in the presence of L-carnitine at the concentrations shown, followed by a 1hr pulse with 500µM H_2O_2, cells were then cultured for a further 48hrs before analysis. The level of apoptosis was determined as described in Figure 4A. Data shown is mean ± SD from one representative experiment (n=4) repeated three times. **B:** LA4 cells were cultured for 24hrs in the presence of L-carnitine at the concentrations shown, some cells were also pulsed with 500µM H_2O_2 for 1hr as indicated, all cells were then cultured for a further 6hrs before analysis. Data shown is the relative MitoSOX fluorescence intensity of treated groups compared to control, mean ± SD, from one representative experiment, n=3-4, repeated twice. For all charts one-way ANOVA following Bonferroni post test was undertaken with **P* < 0.05, ***P* < 0.01, ****P* < 0.001, *****P* < 0.0001 compared to the control group.

Figure 6. Supplementing mice with L-carnitine replenishes lung L-carnitine levels and is accompanied by an improvement in apoptosis levels. Mice were supplemented every second day i.p. with L-carnitine (LC) at a dose of 500mg/kg body weight following a single oropharyngeal administration of PPE, mice were analyzed 28 days later compared to mice that only received PPE or PBS controls. The experiment was repeated twice with n=4-6 mice per group each time. **A:** The concentration of lung specific free L-carnitine normalized to protein levels at 28 days. **B:** Total and differential cell counts in the BALF. **C:** Representative Western Blot and densitometric analysis for cleaved (active)-caspase 3 in lung homogenate of the mice indicated. **D:** Representative photomicrographs of immunohistochemically stained lung sections with anti-cleaved caspase 3 antibody. Positively stained cells in red: open arrow head alveolar epithelial cell, closed arrow head endothelial cell, full arrow airway epithelial cell. Scale bar upper images 100µm, lower images 50µm. Quantification of cleaved caspase 3 positive alveolar epithelial cells using the newCAST system was calculated. Data shown in all charts are the mean values ± SD, with **P* < 0.05, ***P* < 0.01, ****P* < 0.001 and ns not significant, one-way ANOVA following Bonferroni post test.

Figure 7. L-carnitine supplementation improves lung function in PPE-induced emphysematous mice. **A:** Lung function measurements to obtain dynamic compliance, elastance and total lung capacity (TLC) were carried out on day 28 in PBS-treated, PPE-treated and PPE-treated mice supplemented with L-carnitine (LC) every second day at 500mg/kg body weight i.p.. **B:** Representative photomicrographs of H&E stained lung sections from the three groups of mice. Scale bar 200µm. Airspace enlargement was quantified as the mean linear intercept (MLI) by design-based stereology of the H&E stained lung sections using the newCAST system. All data shown are the mean values ± SD from two experiments, n=4-6 per group, one-way ANOVA following Bonferroni post test with ****P < 0.0001 and ns not significant.

Figure 1

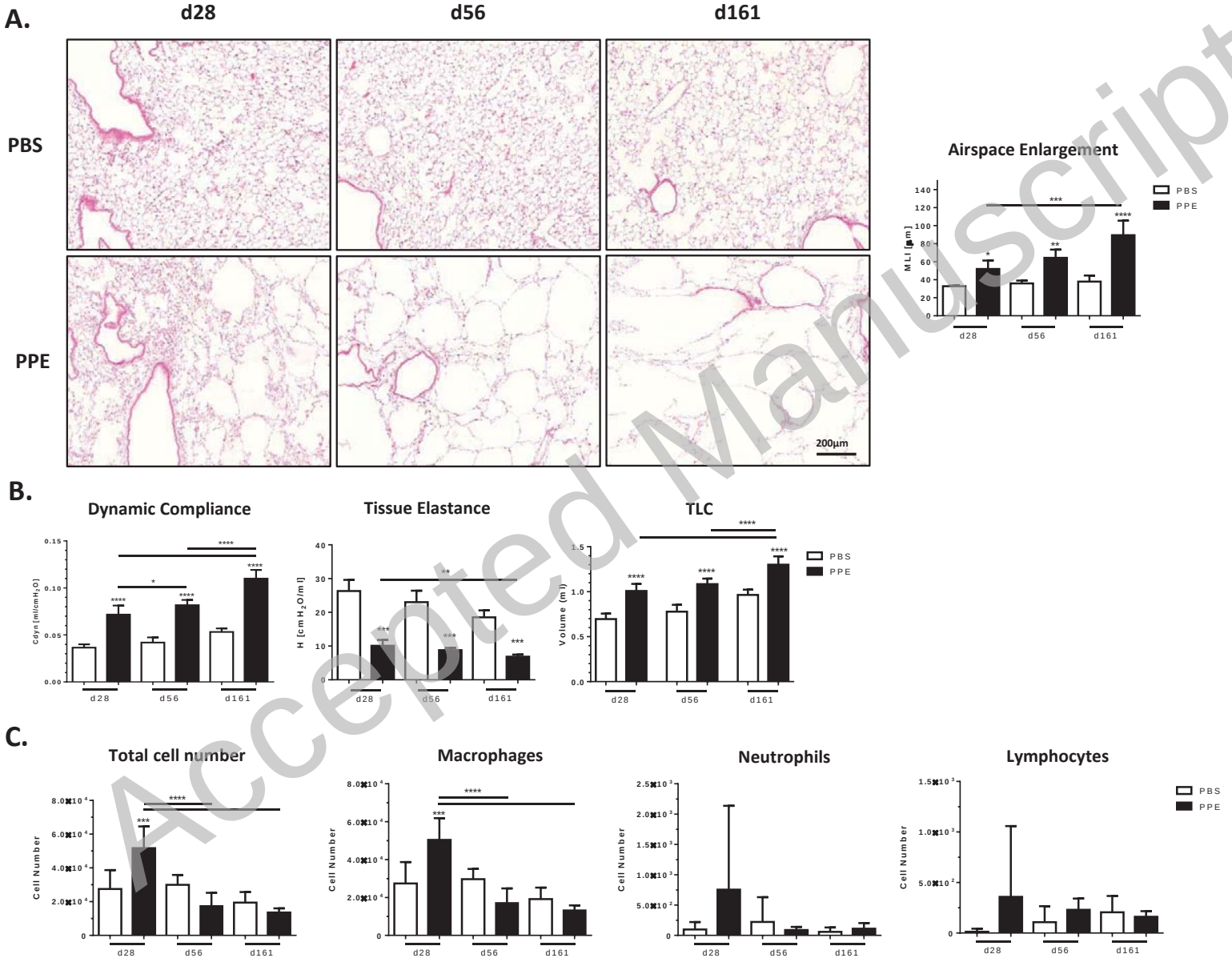

Figure 2

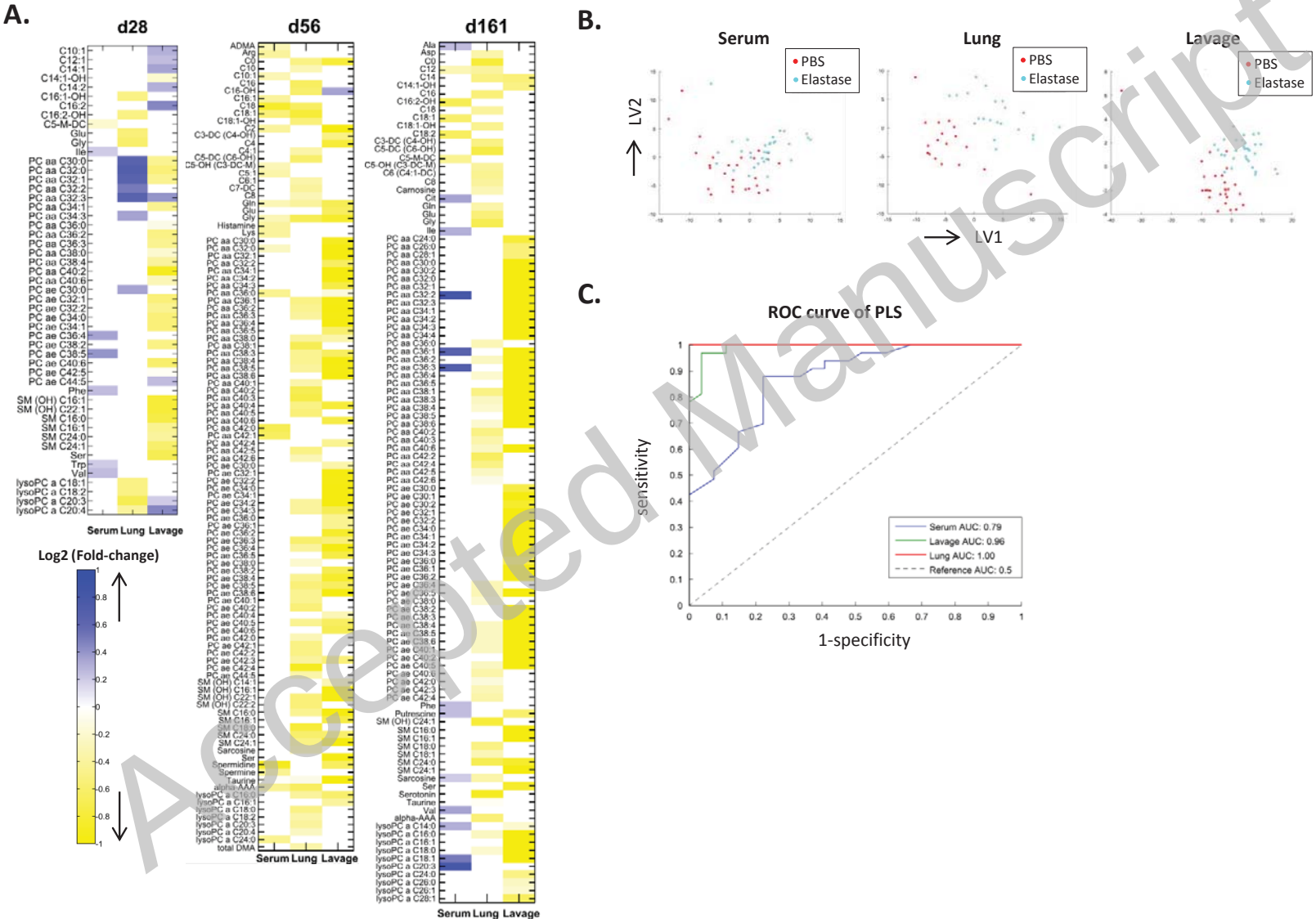

Figure 3

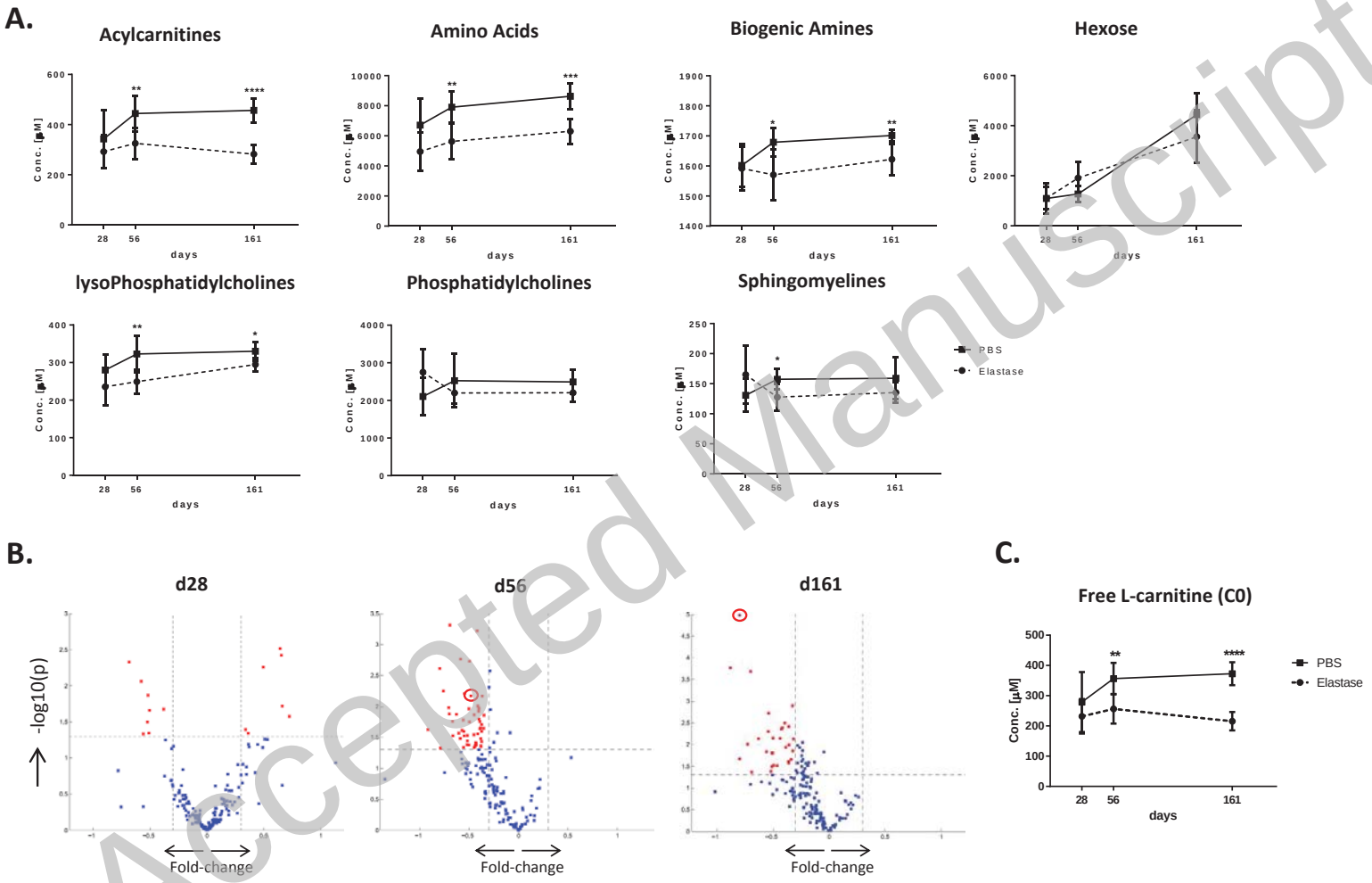

Figure 4

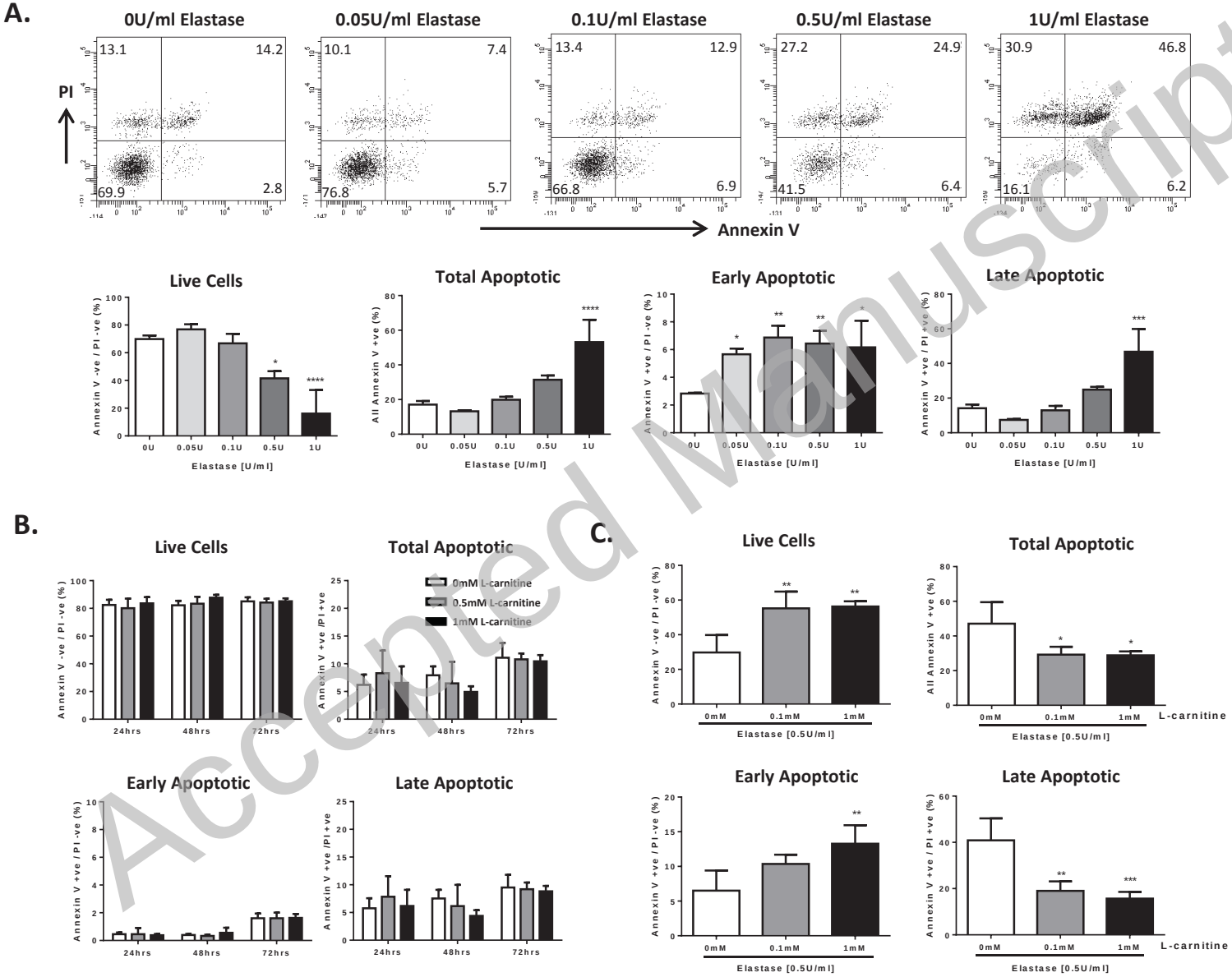

Figure 5

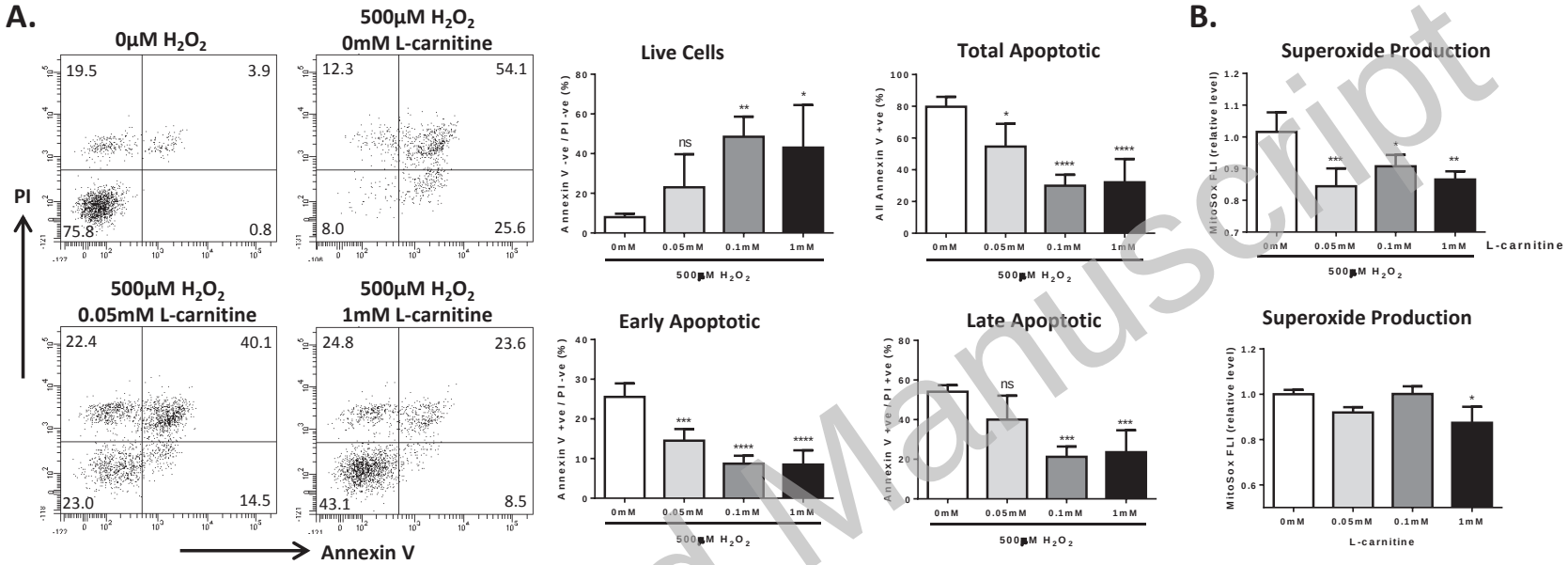

Figure 6

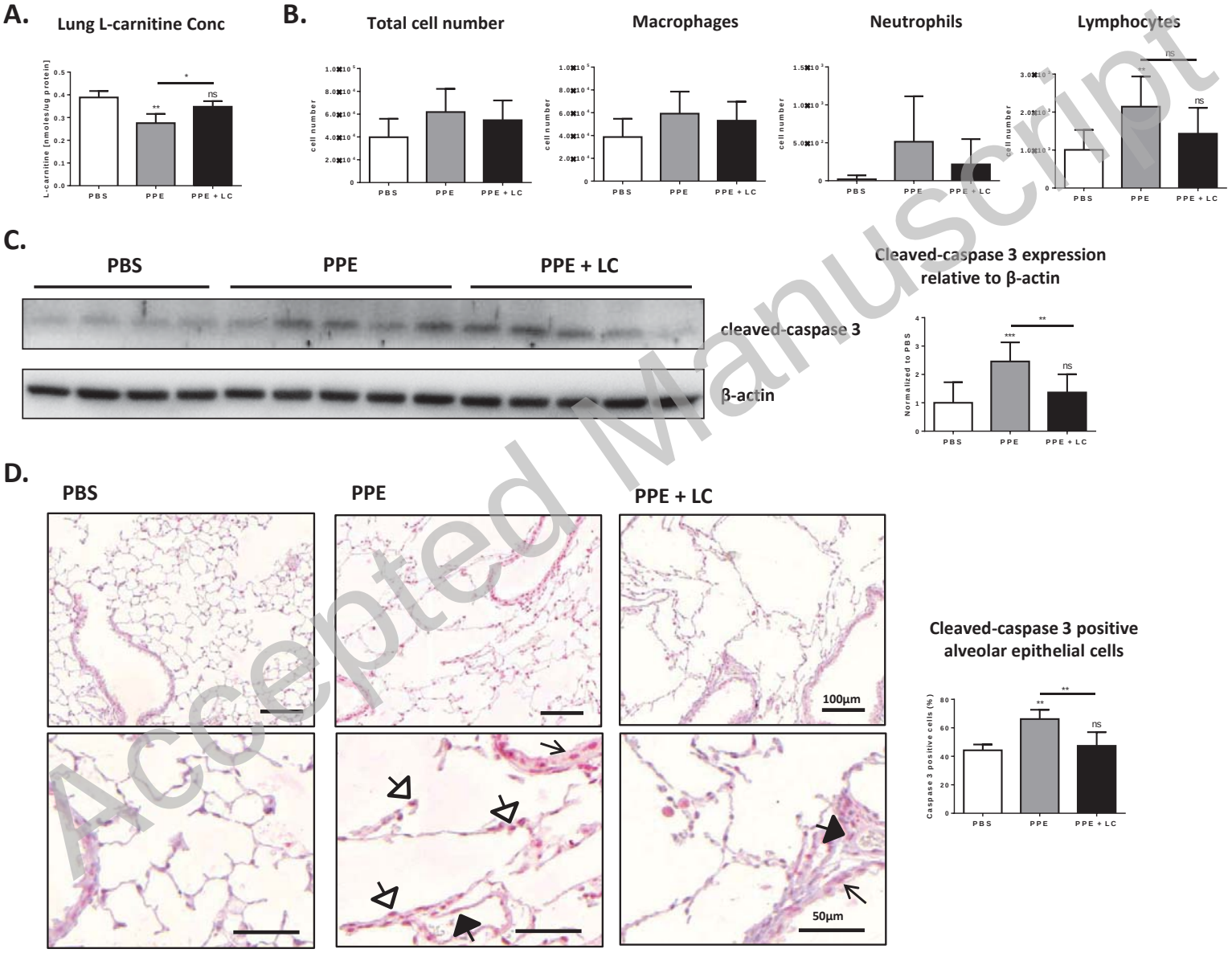

Figure 7